Energy 119 (2017) 1–9

Contents lists available at ScienceDirect

Energy

journal homepage: www.elsevier.com/locate/energy

Effects of catalysts on pyrolysis of castor meal

Guan-Bang Chen [a, *], Yueh-Heng Li [a, b, **], Guan-Lin Chen [c], Wen-Teng Wu [c]

[a] Research Center for Energy Technology and Strategy, National Cheng Kung University, Tainan 701, Taiwan, ROC
[b] Department of Aeronautics and Astronautics, National Cheng Kung University, Tainan 701, Taiwan, ROC
[c] Department of Chemical Engineering, National Cheng Kung University, Tainan 701, Taiwan, ROC

ARTICLE INFO

Article history:
Received 10 June 2016
Received in revised form
10 December 2016
Accepted 18 December 2016

Keywords:
γ-Alumina
Zeolite ZSM-5
Catalyst
Pyrolysis
Castor meal

ABSTRACT

In this study, γ-alumina and zeolite ZSM-5 were used as catalysts to examine their effects on the pyrolysis of castor meal. The operation conditions for the pyrolysis were a pyrolytic temperature of 400 °C, residence time of 120 min, heating rate of 20 °C/min, and nitrogen flow rate of 200 mL/min. With the addition of catalysts, significant variations in pyrolytic products was observed, and the presence of γ-alumina and zeolite ZSM-5 slightly reduced the pyrolytic oil yield. However, the thermal analysis results demonstrate that the catalysts changed the pyrolysis mode and enhanced the hydrogenation/deoxygenation reaction and removed oxygen as CO, CO_2, and H_2O. Gas chromatography-mass spectrometry, elemental analysis, and viscosity analysis were also performed. With the addition of catalysts, the pyrolytic oil consisted of lighter compounds. The viscosity of the pyrolytic oil decreased significantly, and its viscosity index and calorific value increased. Therefore, catalytic pyrolysis can improve the quality of pyrolytic oil, and adding γ-alumina decreases the pyrolysis temperature from 339 °C to 284 °C. In addition, for the deoxygenating ability, the effect of γ-alumina will be greater than that of zeolite ZSM-5.

1. Introduction

According to the International Energy Agency (2015), global energy consumption stratified by power source was 31.1% oil, 28.9% coal/peat, 21.4% natural gas, 10.2% biofuel/waste, 4.8% nuclear, 2.4% hydro, and 1.2% other renewable energy sources such as solar, geothermal, and wind. Currently, global energy supply is largely fossil fuel-based, which has led to the rapid depletion of fossils fuel and a substantial increase in greenhouse gas (GHG) emissions. To mitigate the increase in GHG emissions, improving the efficiency of fossil fuel utilization [1–3] and partially replacing fossil fuels with alternative fuels [4,5] are regarded as feasible and timely measures. Biomass is recognized as a promising ecofriendly alternative source of renewable energy, and it has high availability worldwide. Compared with conventional fossil fuels, biomass generally contains small amounts of sulfur, nitrogen, and ash. Biofuel combustion emits lower amounts of harmful gases such as nitrogen oxides (NO_x) and sulfur dioxide (SO_2), and soot [6]. In addition, the use of biomass fuels provides substantial environmental benefits. Biomass absorbs carbon dioxide during growth and emits it during combustion. Therefore, biomass facilitates atmospheric carbon dioxide recycling and does not contribute to the greenhouse effect.

In terms of converting biomass into biofuel, there are two quintessential methods: biochemical conversion (BCC) and thermochemical conversion (TCC). BCC involves using fermentation and other biological conversion processes to produce biofuels. For example, waste cooking oil is used to produce biodiesel through transesterification, and starchy crops are used to produce bioethanol through fermentation. Biofuels have advantages in storage and transport, as well as versatility in such applications as combustion engines, boilers, turbines, and fuel cells. TCC can be further categorized into direct combustion, gasification, pyrolysis, and liquefaction, and the resulting materials can be used directly as fuels, specialty chemicals, or electricity precursors.

Compared with other biomass-to-energy conversion processes, thermal pyrolysis has attracted more interest from the viewpoint of obtaining liquid fuel product from various biomass species such as woody biomass [7], bagasse [8], straw [9], miscanthus [10], oil palm fiber [11], and municipal solid waste [12,13]. Depending on the operating conditions, pyrolysis can be classified into three main categories: slow, fast, and flash. In addition, the products of pyrolysis processes depend strongly on the heating rate, heating

* Corresponding author.
** Corresponding author. Dept. of Aeronautics and Astronautics, National Cheng Kung University, Tainan 701, Taiwan, ROC.
E-mail addresses: gbchen26@gmail.com (G.-B. Chen), yueheng@mail.ncku.edu.tw (Y.-H. Li).

http://dx.doi.org/10.1016/j.energy.2016.12.070
0360-5442/

temperature, vapor residence time, biomass particle size, and biomass water content. In fast pyrolysis, biomass is generally heated rapidly to a high temperature in the absence of oxygen and yields 60%–75% oily products, 15%–25% solid products, and 10%–20% gaseous products by weight. However, the product yield of biomass pyrolysis can be approximately maximized for charcoal by employing a low-temperature, low-heating-rate process; for liquid products by employing a moderate-temperature, high-heating-rate, short gas-residence-time process; and for fuel gas by employing a high-temperature, low-heating-rate, long gas-residence-time process [14–16].

As to the pyrolysis system, so far, various types of pyrolyzer have been proposed and tested. According to the gas-solid contacting mode, the major designs of pyrolyzer include fixed bed, fluidized bed, entrained bed, rotating cone reactor, ablative reactor, vacuum reactor and so on. Different pyrolyzers have different design configuration and operating characteristics. A brief introduction about these pyrolyzers can be found in the literary work of Basu [17]. In a commercial pyrolyzer, first, a heat-transfer medium is heated up in the reactor. Then it transfers the heat to the feedstock. The heat transfer medium can be the reactor wall (for vacuum reactor), carrier gas (for entrained-bed or entrained-flow reactor) or heat-carrier solids (for fluidized bed) [17].

1.1. Biomass feedstock

Among the various raw materials that can be converted to biomass energy, castor has received considerable attention because of its vitality, ability to grow in barren lands, and excellent soil and water conservation abilities. Castor matures in 6 months, and can be harvested two or three times a year. The oil content of castor seeds is more than 50%, and the annual output of castor oil can reach 10–15 tons per hectare. Fig. 1 shows the castor seeds, which are provided by the Asian Green Energy company, and the castor meals is used in the study. Castor is currently one of the world's top ten oil crops, and its main distribution areas include Africa, South America, Asia, and Europe, with castor seed production in India, China, and Brazil accounting for 81.2% of the global total. Castor seeds are oval-shaped (Fig. 1) and divided into two parts: the kernel and the shell. The kernel accounts for approximately 70%–75% of the total weight of a seed. Castor seeds are rich in oil and have thus been referred to as “green renewable petroleum.” Castor oil can be extracted under pressure, with or without heating, or by using solvents [18]. Castor oil is a critical industrial raw material, with the international market concentrated mainly in North America, Europe, and China. The residue left after the oil has been pressed out of the castor seeds is called castor meal, and it is an abundant biomass feedstock.

Fig. 1. Photograph of castor seeds.

Castor oil is generally obtained by squeezing castor seeds, a process that can be accomplished via either cold or hot pressing. With cold pressing, castor oil is obtained without steam heating. With this approach, the resulting castor oil is not exposed to high temperatures, and thus its medicinal properties are preserved. By contrast, with hot pressing, castor oil is obtained through steam heating. A slow heat treatment process can reduce the viscosity of the residual castor oil, thus rendering it possible to extract oil that could not be obtained through cold pressing alone [19]. However, conventional squeezing methods have some limitations, and we demonstrated in a previous study [20] that castor meal retains a certain amount of oil.

1.2. Catalysts in pyrolysis

In addition to increasing the reaction rate and yield, catalysts are employed in biomass pyrolysis to improve product quality. Catalysts are used to enhance pyrolysis reaction kinetics through the cracking of higher molecular weight compounds into lighter hydrocarbon products [21]. In addition, introducing an appropriate catalyst to a biomass pyrolysis process can boost the biomass conversion efficiency, reduce tar formation, and increase the target product yield. Pyrolytic oil obtained from biomass cannot be applied directly as fuel because it is corrosive, has high viscosity, and low heating value. Deoxygenation and moisture content reduction are often performed to improve the quality of pyrolytic oil [22,23]. Two methods have been applied to reduce the oxygen content of pyrolytic oil: hydrogenation with high-pressure hydrogen and carbon monoxide, and using catalysts (zeolite, Si–Al, molecular sieves) to promote pyrolysis at atmospheric pressure. The second method is used extensively in industry because of the following advantages: (1) no hydrogen is used; (2) the process takes place at atmospheric pressure, which means decreased costs; and (3) the operating temperature is analogous to the desired temperature for bio-oil production.

Babich et al. studied the pyrolytic conversion of chlorella algae to a liquid fuel precursor in the presence of a catalyst (Na_2CO_3) [24]. Thermogravimetric analysis (TGA) showed that adding Na_2CO_3 influenced the primary conversion of chlorella by decreasing the decomposition temperature. In the presence of Na_2CO_3, the pyrolytic gas yield increased and the pyrolytic liquid yield decreased at a given pyrolysis temperature. However, the higher heating value, higher aromatic content, and lower acidity of the obtained pyrolytic oil show promise for the production of high-quality bio-oil from algae through catalytic pyrolysis.

Pütün studied the pyrolysis of cotton seeds in a tubular fixed-bed reactor under various sweeping gas (N_2) flow rates and various pyrolysis temperatures [25]. Without a catalyst, the maximum available bio-oil yield was approximately 48.3 wt% at 550 °C and a nitrogen flow rate of 200 mL/min. Under the optimum conditions, biomass samples were catalytically pyrolyzed with various amounts of MgO catalyst (5 wt%, 10 wt%, 15 wt%, and 20 wt% of raw material). Experimental results indicated that the presence of the catalyst decreased the bio-oil yield but improved its quality in terms of heating value, hydrocarbon distribution, and the removal of oxygenated groups. Moreover, adding greater amounts of catalyst lowered the bio-oil yield but raised the yield of gas and char.

Wang et al. investigated the pyrolysis of herb residue in a fixed-bed reactor to determine the effects of pyrolysis temperature and

catalysts (ZSM-5, Al-SBA-15, and alumina) on product yield and bio-oil quality [26]. The maximum bio-oil yield of 34.26 wt% was obtained with the addition of 10 wt% alumina at a pyrolysis temperature of 450 °C. The presence of a catalyst decreased the oxygen content of the resulting bio-oil and increased its calorific value. The order of catalyst effectiveness in improving pyrolytic oil quality was in the order of Al_2O_3 > Al-SBA-15 > ZSM-5. The bio-oil with the lowest oxygen content (26.71%) and highest heating value (25.94 MJ/kg) was obtained with 20 wt% Al_2O_3.

Shadangi et al. investigated pyrolysis of Niger seed with and without the catalysts of Al_2O_3, CaO and Kaolin [27]. With the presence of catalysts, the oil yield was decreased marginally, but the fuel properties were enhanced compared with thermal pyrolysis. They also performed thermal and catalytic pyrolysis of Karanja seed with these three kinds of catalyst [28]. The optimum temperature was 550 °C for thermal pyrolysis to produce the maximum liquid yield (33% for oil and 22.17% for aqueous product by weight). The pyrolytic oil yield of catalytic pyrolysis with Al_2O_3 and Kaolin was better than that of thermal pyrolysis. In addition, all the catalysts improved the quality of pyrolytic oil in comparison with thermal pyrolysis. Koul et al. studied the effect of catalytic vapor cracking of castor seed with the catalysts of Kaolin, CaO and ZnO [29]. The cracking of castor seed pyrolytic vapor over the catalyst bed was verified to improve the fuel properties of pyrolytic oil for all catalysts. It found that CaO and Kaolin had significant influence on the viscosity, pH, calorific value and pour point of pyrolytic oil.

As mentioned, adding a catalyst can promote biomass pyrolysis kinetics and improve the quality and yield of the resulting pyrolytic products. In a previous study, we used the Taguchi method to investigate the process of thermal pyrolysis of castor meal to achieve the maximum pyrolytic oil yield [20]. The effects of pyrolytic temperature, residence time, heating rate, and nitrogen flow rate on castor meal pyrolysis were investigated [20]. The maximum pyrolytic oil yield was obtained under the following operating conditions: pyrolysis temperature of 400 °C, residence time of 120 min, heating rate of 20 °C/min, and nitrogen flow rate of 200 mL/min. On the basis of these results, in the present study, γ-alumina and zeolite ZSM-5 were used as catalysts to investigate their effects on the pyrolysis of castor meal. In addition, we addressed the characteristics of the resulting pyrolytic oil.

2. Experimental apparatus

The experimental setup for the pyrolysis of castor meal is shown in Fig. 2. We mixed 50 g of castor meal uniformly with the catalyst and packed the mixture in a cylindrical metal holder. Two commercial catalysts, namely γ-alumina and zeolite ZSM-5, were used in the pyrolysis experiments. Three mass ratios of catalyst/castor meal were engaged, 1%, 5%, and 10%, respectively. The pyrolysis conditions were the pyrolytic temperature of 400 °C, residence time of 120 min, heating rate of 20 °C/min, and the nitrogen flow rate of 200 mL/min. Aluminum oxide (γ-alumina) is an activated and neutral powder with a particle size of 100–120 μm, pore size of 58 Å, and specific surface area of 155 m^2/g, whereas zeolite ZSM-5 is an aluminosilicate mesostructured powder with a Si/Al molar ratio of 40, specific surface area of 425 m^2/g, and acidity of 0.2 mmol/g. The catalysts were provided by ECHO Chemical Co., Ltd. In addition, the catalyst acidity was determined by Ammonia Chemisorption (ASTM D4824). The holder was made of stainless steel 316, which is highly resistant to pitting and crevice corrosion. Hence, it did not react chemically with the pyrolytic product during the procedure. The holder was placed in a tube furnace (F21135, Thermolyne, 120 V/1.35 KW), which was evacuated using a vacuum pump (MZ 2C, Vacuubrand) and then filled with nitrogen to ambient pressure. The operating temperature of tube furnace ranges from 100 °C to 1200 °C, and its uniformity is approximately ±3 °C over the effective tube length of 15.2 cm. The furnace was heated to the target temperature, which was maintained throughout the pyrolysis process. The high-temperature volatile gas generated by the biomass pyrolysis process was delivered to a condensing system for forming liquid products. The pyrolytic liquid consisted of organic part (pyrolytic oil) and aqueous matter. Pyrolytic oil was then separated from the aqueous products by using a separatory funnel. The remaining gas that could not be condensed was discharged through the exhaust system. After the furnace cooled to room temperature, the holder was removed. The remaining material in the holder was castor meal char. Since the mass of pyrolytic liquid and castor meal char can be directly collected and gauged, the mass of discharged bio-gas can be determined on the basis of the mass conversion.

Thermal analysis (SDT Q600, TA Instruments) was performed through TGA and differential scanning calorimetry (DSC) simultaneously. The abovementioned device was also connected to a Fourier transform infrared (FTIR) spectrometer (Tensor 27, Bruker) for synchronization. The temperature range of the thermal analysis was set to 50 °C–1000 °C; the heating rate was 10 °C/min. The test sample was placed in a 90-μL platinum crucible, and the nitrogen or air flow rate was set to 100 mL/min. The FTIR scanning process was set to 64, and the wavenumber ranged from 650 to 4000 cm^{-1} with a resolution of 1 cm^{-1}. Thermal analysis of the castor meal and qualitative analysis of the pyrolytic gas products were performed to determine the effects of the catalysts on castor meal pyrolysis.

The FTIR spectrometer (Nicolet, Magna-IR 560 Spectrometer) was used to qualitatively analyze the liquid sample. The scanning process was set to 64, and the scan ranged from 500 to 4000 cm^{-1} with a resolution of 22 cm^{-1}. The liquid sample was dropped on a

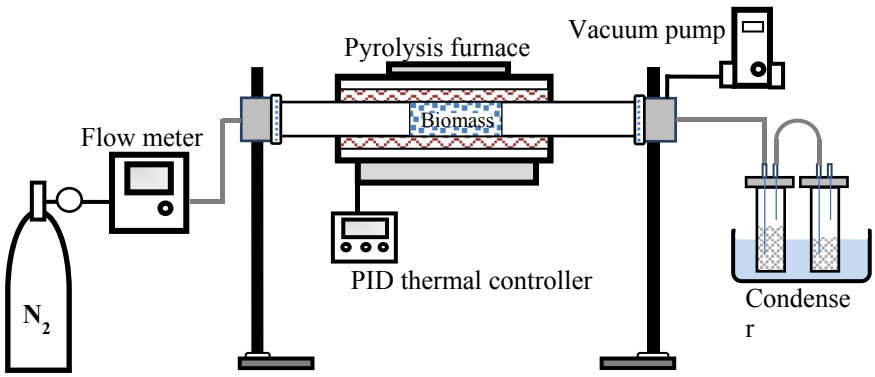

Fig. 2. Experimental setup for pyrolysis.

KBr plate and then placed in the spectrometer for characterization. A dynamic rheometer (RS-150, Haake) was used to measure the viscosity of the pyrolytic oil obtained from castor meal with and without catalysts at 25 °C. In addition, the viscosities at 40 °C and 100 °C were measured to calculate the viscosity index. An element analyzer (VarioEL III) was used to verify the carbon, hydrogen, oxygen, nitrogen, and sulfur content of the pyrolytic oil on a weight basis.

An Agilent 7890A-5975C gas chromatograph equipped with an Agilent 5973 mass-selective detector was used to determine the composition of the pyrolytic oils obtained with and without catalysts. HP-5ms GC Column was used and the oven temperature was initially programmed at 40 °C for 5 min. Then it was increased to 300 °C at the heating rate of 20 °C/min, and the oven temperature was maintained at 300 °C for 20 min. The sample injection volume of single shot was 0.2 μL. Helium was delivered as the carrier gas with the flow rate of 1 mL/min. For the mass-selective detector, the operating conditions were specified in the scan range of 15–550 Da, source temperature of 230 °C, and ionization voltage of 70 eV.

3. Results and discussion

3.1. Catalytic TGA of castor meal

Fig. 3 shows the TGA thermographs of castor meal with γ-alumina and zeolite ZSM-5 catalysts obtained at a heating rate of 10 °C/min and a nitrogen flow rate of 100 mL/min. The ratio of catalyst to castor meal is fixed 10% in the TGA experiment. The solid and the dashed curves represent TGA and DTG data, respectively. The blue curves denote the thermal pyrolysis; the red curves denote catalytic pyrolysis with γ-alumina and the green lines denote catalytic pyrolysis with zeolite ZSM-5.

The DTG curves in Fig. 3 show that the maximum mass loss occurred at 339 °C without a catalyst. When zeolite ZSM-5 was present, the maximum mass loss occurs at 342 °C. These two peaks occur at similar temperatures, indicating that zeolite ZSM-5 did not significantly influence the pyrolysis temperature. However, when γ-alumina was used as the catalyst, the major pyrolysis peak occurred at 284 °C. Notably, γ-alumina reduced the pyrolysis temperature by approximately 55 °C, and the pyrolysis process generated two identical peaks. Because γ-alumina has a large pore structure, the first peak represents pyrolysis reactions that occur mainly on the catalyst surface, and the second peak denotes pyrolysis reactions occurring within the catalyst pores. Analogously, Xu et al. discovered two-peak catalytic pyrolysis reactions for wastewater sludge when using alumina as the catalyst [30].

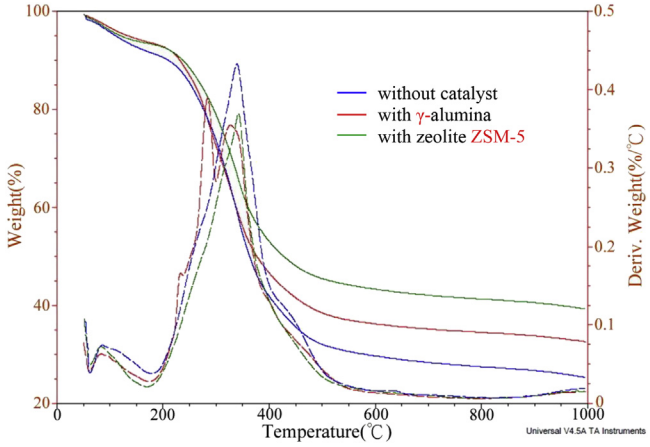

Fig. 3. TGA results of castor meal with two catalysts (N_2 flow rate: 100 mL/min; heating rate: 10 °C/min).

In the present study, the TGA equipment was connected to the FTIR spectrometer to analyze the composition of the resulting pyrolytic gas. Light gases such as CO_2, CO, H_2O, and CH_4 can be detected easily. However, for more complex compounds, such as hydrocarbons, phenols, acids, and carbon-based compounds (acids, aldehydes, and ketones), only special functional groups can be identified. Fig. 4 shows three-dimensional images of the FTIR signals for castor meal with the two catalysts. The addition of a catalyst (γ-alumina or zeolite ZSM-5) shifted the pyrolysis mode. In the early stage, within 3000 s, the catalyst caused a significant increase in H_2O (O–H stretching vibration, 3731 cm^{-1}), CH_4 (C–H stretching vibration, 3014 cm^{-1}), CO_2 (C═O stretching vibration, 2458 cm^{-1}), CO (C–O stretching vibration, 2181 cm^{-1}), and phenol (O–H bending vibration, 1278 cm^{-1}), particularly when γ-alumina was used as the catalyst. The catalyst enhanced the secondary reactions, and the volatile substances were further decomposed into smaller hydrocarbon molecules. Thus, catalytic pyrolysis can remove oxygen atoms and convert volatile substances into the three molecules, namely, H_2O, CO, and CO_2, and improve the quality of pyrolytic oil.

3.2. Effects of amount of catalyst on production of pyrolytic products

Figs. 5 and 6 show the effects of the amounts of the two catalysts (zeolite ZSM-5 and γ-alumina) on the pyrolysis product yield obtained from castor meal. The blue line with diamonds, green line with triangles, orange line with rectangles, and black line with circles represent castor meal char production and yields of pyrolysis liquid, pyrolysis gas, and pyrolytic oil, respectively.

As shown in Fig. 5, the pyrolytic liquid yield for various catalytic ratios was constant at approximately 37%. Compared with pyrolytic liquid production in the case without catalysts, the pyrolytic liquid yield in the case with 10 wt% zeolite ZSM-5 showed no significant change. Nonetheless, the pyrolytic oil yield decreased slightly from 19.6% in the case without catalysts to 16% in the case with 10 wt% zeolite ZSM-5. Consequently, the percentage of aqueous substances increased with the catalytic ratio, whereas the percentage of pyrolytic liquid remains approximately constant. Wang et al. studied the catalytic pyrolysis of herb residue and found that the acidity and smaller pores of zeolite promote the production of char [26]. This finding is analogous to the results of catalytic pyrolysis of castor meal in the current study. The yield of castor meal char increased from 36% in the case without a catalyst to 40% in the case with 10 wt% zeolite ZSM-5.

Fig. 6 shows that the production of castor meal char decreased slightly with increasing amounts of γ-alumina catalyst. The yield of pyrolytic liquid first decreased and then increased with an increase in the amount of γ-alumina catalyst, whereas the yield of pyrolytic oil decreased. The pyrolytic oil yield decreased from 19.6% in the case without catalysts to 15% in the case with 10 wt% γ-alumina. Presumably, the percentage of the aqueous phase in pyrolytic liquid increased significantly. The γ-alumina can induce the aforementioned secondary chemical reactions (in which pyrolytic substances are further reduced to smaller molecules), thereby increasing the yield of pyrolytic gases from 25% without a catalyst to approximately 28% with 10 wt% γ-alumina.

3.3. TGA burning profile of castor meal char

Fig. 7 shows the TGA burning profile of castor meal char obtained at a heating rate of 10 °C/min and an air flow rate of 100 mL/

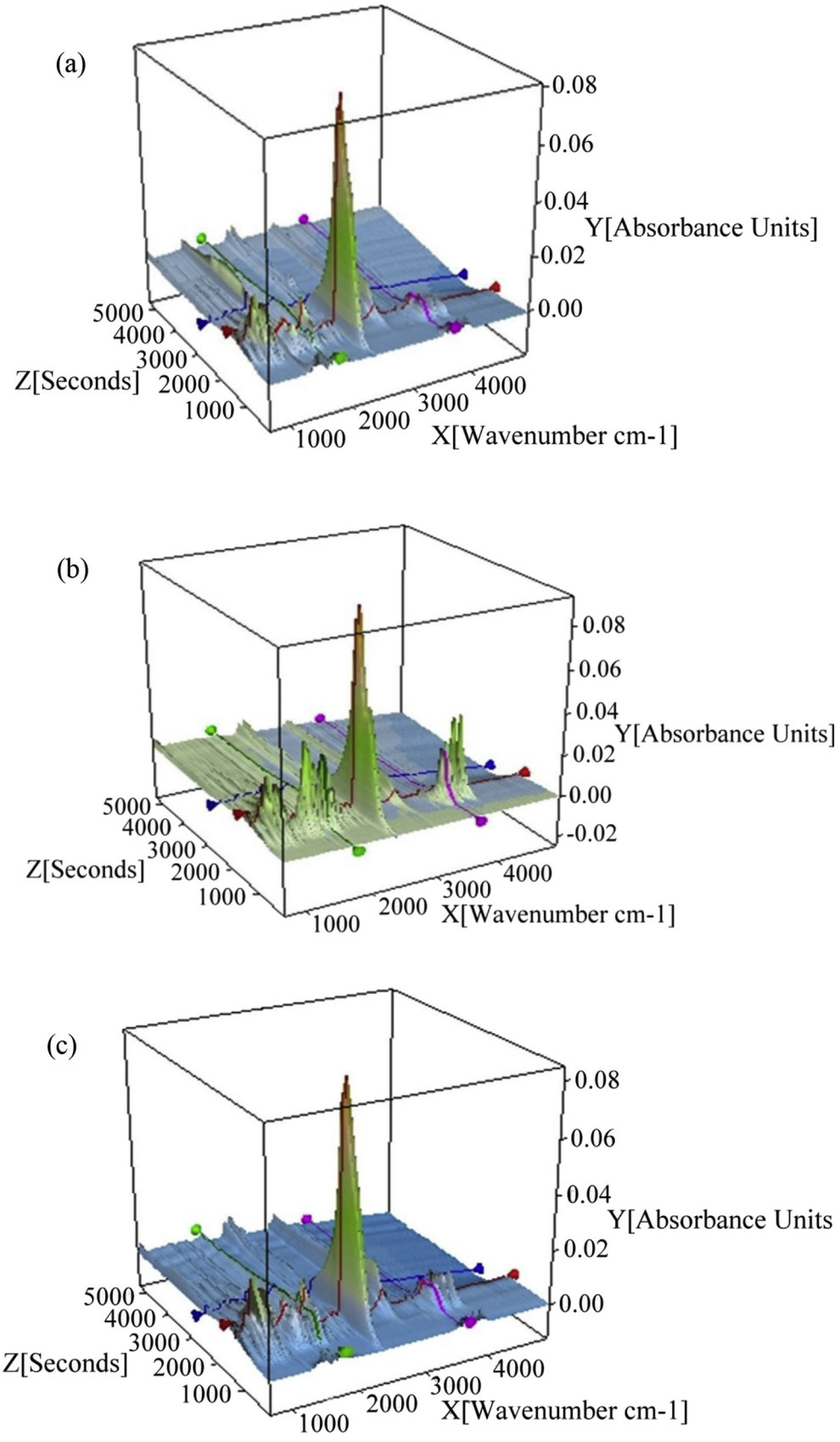

Fig. 4. FTIR spectra of the pyrolytic gas of castor meal (a) without a catalyst, (b) with γ-alumina, and (c) with zeolite ZSM-5.

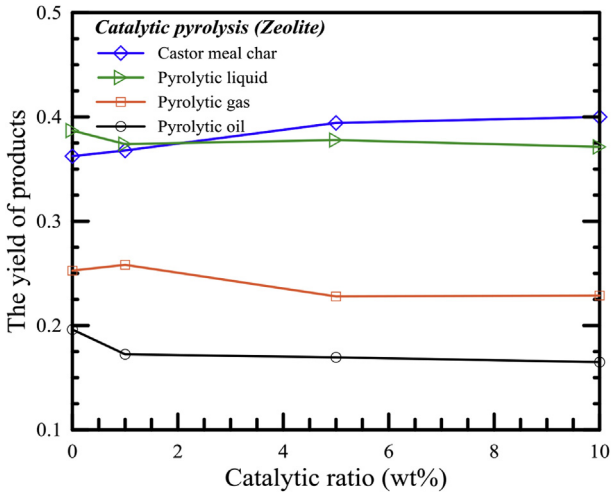

Fig. 5. Effect of the amount of zeolite ZSM-5 on the pyrolytic product yield.

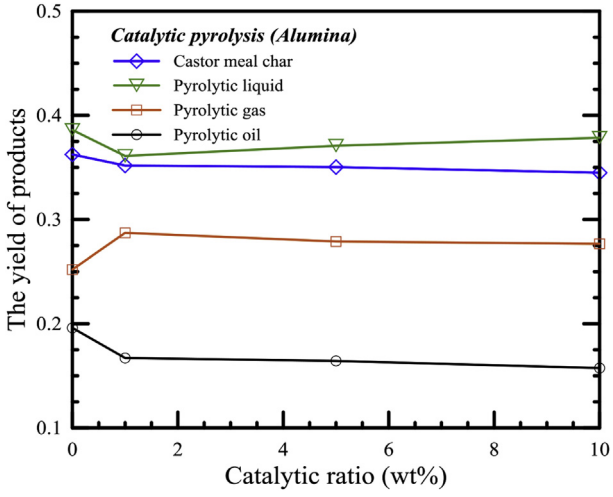

Fig. 6. Effect of the amount of γ-alumina on the pyrolytic product yield.

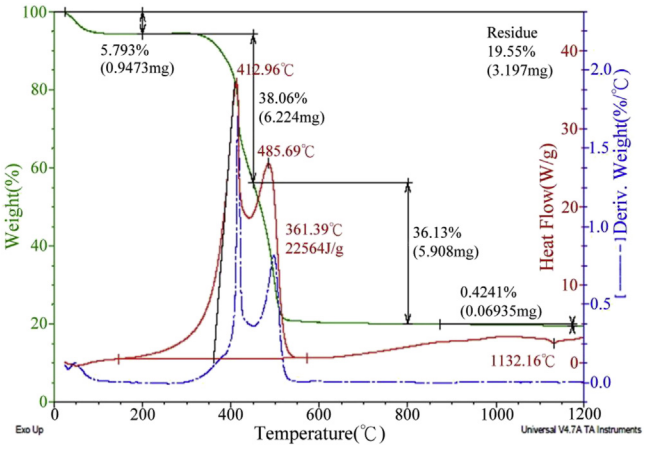

Fig. 7. TGA burning profile of castor meal char (air flow rate: 100 mL/min; heating rate: 10 °C/min).

min. The castor meal char is the solid product from the pyrolysis of castor meal. The green curve represents TGA data, the blue curve represents differential thermogravimetry (DTG) data, and the red curve represents DSC data. The figure shows that the main reaction occurred between 200 °C and 550 °C. The figure also shows two distinct peaks in the DTG and DSC curves. In the DTG and DSC curves, two primary reactions occur at operating temperatures of 413 °C and 485 °C, respectively. Morgan et al. found that a considerable proportion of two media containing charcoal macerals produced two distinct peaks in a thermal analysis [31]. The first major peak represents coal vitrinite combustion, accounting for approximately 38.06% of mass loss. The second peak represents coal inertinite combustion, accounting for approximately 36.13% of mass loss. Moreover, integration of the DSC curve yields a heating value of 22.564 MJ/kg for castor meal char. After the castor meal char is burnt, about 19.55% of the mass remains as residue.

3.4. TGA burning profile of pyrolytic oil

Fig. 8 shows the TGA burning profile of pyrolytic oil obtained from castor meal at a heating rate of 10 °C/min and an air flow rate of 100 mL/min. The green curve represents TGA data, the blue curve represents DTG data, and the red curve represents DSC data. The combustion of the castor pyrolytic oil inhibited multistage reactions, and weight loss occurred mainly between 200 °C and 300 °C. The first stage of the TGA curve presents a weight loss of 10.51%, which can be ascribed to removal of the water from the castor meal. In contrast to the castor meal char, the heating value of the castor pyrolytic oil could not be estimated by integrating the DSC curve because the volatile substances in pyrolysis oil do not burn out before being removed from the reactor by carrying air. Consequently, the heating value of the castor pyrolytic oil was lower than the real value. After the castor pyrolytic oils were burned, only 0.049% of the total mass remained as residue. Accordingly, the application of castor pyrolytic oil in a combustion system would ameliorate coking more effectively than the application of heavy fossil fuels would.

3.5. Analysis of components of pyrolytic oil

The concentrations of the top 10 organic constituents of the pyrolytic oils with and without catalysts are listed in Table 1. The major component of the pyrolytic oils in the three cases is oleamide. Fatty acid methyl esters are mainly 7, 10-hexadecadienoic acid methyl ester ($C_{17}H_{30}O_2$) and linoleic acid methyl ester ($C_{19}H_{34}O_2$). To examine the effects of the catalysts on pyrolytic oil formation, the components of the pyrolytic oil were accumulated

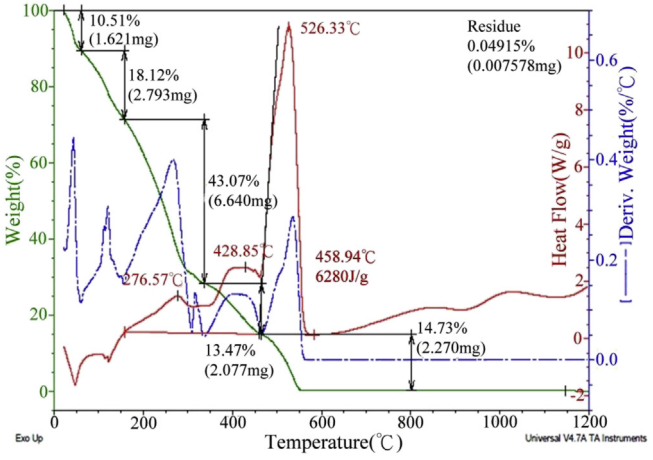

Fig. 8. TGA burning profile of the pyrolytic oil obtained from castor meal (air flow rate: 100 mL/min; heating rate: 10 °C/min).

Table 1
Ten main compositions of castor pyrolytic oils.

Case without catalyst		Case with 5 wt% zeolite ZSM-5		Case with 5 wt% γ-alumina	
Component	Area (%)	Component	Area (%)	Component	Area (%)
9-Octadecenamide ($C_{18}H_{35}NO$)	21.3	9-Octadecenamide ($C_{18}H_{35}NO$)	11.06	9-Octadecenamide ($C_{18}H_{35}NO$)	19.57
11-Nitro-1-Undecene ($C_{11}H_{21}NO_2$)	8.84	Octadecenamide ($C_{18}H_{35}NO$)	7.87	11-Nitro-1-Undecene ($C_{11}H_{21}NO_2$)	8.56
13-Octadecenal ($C_{18}H_{34}O$)	7.17	11-Nitro-1-Undecene ($C_{11}H_{21}NO_2$)	7.16	1,E-11,Z-13-Heptadecatriene ($C_{17}H_{30}$)	5.02
7,10-Hexadecadienoic acid, methyl ester ($C_{17}H_{30}O_2$)	3.79	1,E-11,Z-13-Octadecatriene ($C_{18}H_{32}$)	4.67	Benzo-2,3-pyrrole (C_8H_7N)	3.67
3-Hexadecanol ($C_{16}H_{34}O$)	3.45	Benzo-2,3-pyrrole (C_8H_7N)	3.94	7,10-Hexadecadienoic acid, methyl ester ($C_{17}H_{30}O_2$)	3.45
Benzo-2,3-pyrrole (C_8H_7N)	3.26	7,10-Hexadecadienoic acid, methyl ester ($C_{17}H_{30}O_2$)	3.7	1,E-8,Z-10-Hexadecatriene ($C_{16}H_{28}$)	3.11
p-Cresol (C_7H_8O)	2.98	Phenol (C_6H_6O)	3.44	p-Cresol (C_7H_8O)	2.89
Cycloalkene Ketone ($C_8H_{12}O$)	2.66	Linoleic acid methyl ester ($C_{19}H_{34}O_2$)	3.27	Octadecenamide ($C_{18}H_{35}NO$)	2.8
2-Heptadecynoic acid ($C_{17}H_{30}O_2$)	2.63	Cyclo-(leucyl-prolyl) ($C_{11}H_{18}N_2O_2$)	2.88	Linoleic acid methyl ester ($C_{19}H_{34}O_2$)	2.58
Phenol (C_6H_6O)	2.29	1,E-11,Z-13-Heptadecatriene ($C_{17}H_{30}$)	2.84	Phenol (C_6H_6O)	2.47

and divided into three regions: low-carbon-number compounds (C5-C12), middle-carbon-number compounds (C13-C17), and high-carbon-number compounds (≥C18). The results are shown in Table 2. Without a catalyst, the proportions of low-, middle-, and high-carbon-number compounds were approximately 36.14%, 22.19%, and 34.86%, respectively. Adding 5 wt% catalyst (zeolite ZSM-5 or γ-alumina) significantly increased the proportions of low- and middle-carbon-number compounds. The effect of the zeolite ZSM-5 catalyst was particularly obvious, as the ratios of low- and middle-carbon-number compounds increased from 36.14% to 40.84% and from 22.19% to 29.73%, respectively. This shows that adding catalysts in pyrolysis of castor meal facilitates the decomposition of high-carbon-number pyrolytic oil into low-carbon-number pyrolytic oil. Dũng et al. used zeolite-series catalysts for the pyrolysis of waste tires and found that the catalyst led to the production of greater amounts of lower-carbon-number hydrocarbon compounds [32]. This explains how the catalytic reaction can decompose high-carbon-number hydrocarbons to low-carbon-number hydrocarbons.

3.6. Viscosity analysis of pyrolytic oil

The viscosity and viscosity index of pyrolytic oil were analyzed. The viscosity and viscosity index values of squeezed castor oil and castor pyrolytic oil are shown in Table 3. High oil viscosity implies a stronger oil film, whereas low viscosity indicates better mobility. A higher viscosity index means that temperature has a smaller effect on viscosity, and thus the oil can be applied over a wider temperature range. The value of viscosity index less than 100 was calculated according to ASTM D2270(A), and the remaining values were calculated according to ASTM D2270(B). These two standards are described as follows:

(1) Viscosity index <100:

$$\text{Viscosity index of target oil} = (L - U)/(L - H) \times 100, \quad (1)$$

where H is the viscosity of standard oil at a viscosity index of 100 at 100 °F, L is the viscosity of standard oil at a viscosity index of 0 at 100 °F, and U is the viscosity of the target oil at 100 °F.

(2) Viscosity index >100:

$$\text{Viscosity index of the target oil} = [(\text{antiLogN}) - 1/0.0715] + 100, \quad (2)$$

where N is the viscosity of the target oil at 210 °F resulting in the equivalent viscosity of H and U at 100 °F; that is, N = (log H − log U)/(log KV210) or KV210 = H/U (3). Here, KV210 denotes the kinematic viscosity of the target oil at 210 °F.

Table 3 shows that the viscosity of the castor pyrolytic oil is 4.37 Pa s and that of squeezed castor oil is 0.477 Pa s. The viscosity of the pyrolytic oil is significantly higher than that of the squeezed castor oil. In addition, the viscosity index of the castor pyrolytic oil is presumably higher than that of the squeezed castor oil. Therefore, castor pyrolytic oil could be alternatively used as a lubricant.

Table 3 shows that adding catalysts increased the viscosity index of the castor pyrolytic oil. When 5 wt% γ-alumina or zeolite ZSM-5 catalyst was added in the pyrolysis process, the viscosity index of the resulting bio-oil increased from 643 (without a catalyst) to 689 (γ-alumina case) and 737 (zeolite ZSM-5 case). Therefore, catalytic pyrolysis can improve the high-temperature tolerance of the resulting bio-oil by broadening its operating range. In addition, catalytic pyrolysis significantly reduced the viscosity of the castor pyrolytic oil. In the catalytic pyrolysis process with the addition of 5 wt% catalysts, the viscosity decreased from 4.37 Pa s (without a catalyst) to 2.885 Pa s (γ-alumina case) and 2.929 Pa s (zeolite ZSM-5 case), respectively. The γ-alumina and zeolite ZSM-5 can induce catalytic cracking in pyrolysis; that is, it can break down heavy hydrocarbons into light hydrocarbons. This contributes toward reducing the viscosity of pyrolytic oil and enhancing its fluid mobility.

Table 2
Results of the carbon number analysis of castor pyrolytic oil.

Case	C_5–C_{12} (%)	C_{12}–C_{17} (%)	>C_{18} (%)
Without catalyst	36.14	22.19	34.86
With 5 wt% γ-alumina	40.68	21.15	31.72
With 5 wt% zeolite ZSM-5	40.84	29.73	28.43

3.7. Elemental composition and heating values of catalytic pyrolysis products

The heating value is a crucial parameter of biomass fuel quality. The heating values of pyrolytic oil can be calculated using an empirical equation and the empirical equation functions of the main chemical elements such as C, H, O, N, and S. The element values of pyrolytic oil can be determined through an elemental analysis. The following frequently cited equation for fuel liquids was developed by Lloyd and Davenport by using a regression model with 138 compounds representative of the substances found in fossil fuels [33]:

Table 3
Viscosity and viscosity indices for squeezed castor oil and castor pyrolytic oil.

	Pressed oil	Pyrolytic oil (without catalyst)	Pyrolytic oil (with 5 wt% γ-alumina)	Pyrolytic oil (with 5 wt% zeolite ZSM-5)
Viscosity (Pa s at 25 °C)	0.477	4.370	2.885	2.929
Viscosity Index (VI)	603	643	689	737

$$\text{Calorific value (Lloyd–Davenport, kJ/kg)} = 357.77 \times C + 917.58 \times H - 84.51 \times O - 59.38 \times N + 111.87 \times S \quad (4)$$

Table 4 shows the elemental composition and heating values of pyrolytic oil obtained from castor meal. Adding γ-alumina and zeolite ZSM-5 as catalysts led to the same increasing trends in the variation of the proportions of N, C, H, and O. The addition of 5 wt% catalyst increased the ratio of H from 6.24% (without a catalyst) to 8.99% (γ-alumina case) and 8.33% (zeolite ZSM-5 case); the ratio of O decreased from 22.3% (without a catalyst) to 20.43% (γ-alumina case) and 20.75% (zeolite ZSM-5 case). According to the TGA and FTIR results, both γ-alumina and zeolite ZSM-5 enhanced the deoxygenation reaction. Oxygen in pyrolytic oil was removed as CO, CO_2, and H_2O, thereby increasing the heating value of the pyrolytic oil. With the addition of 5 wt% catalyst, the heating value of the castor pyrolytic oil increased from 22.277 MJ/kg (without a catalyst) to 25.882 MJ/kg (γ-alumina case) and 24.493 MJ/kg (zeolite ZSM-5 case).

Zeolite ZSM-5 can filter large O compounds, mainly because of its acidity and small pores. The γ-alumina has large pores, allowing both long- and short-chain molecules to reach the internal surface. The internal surface is covered with many active sites, and the adsorbed molecules are accelerated for oxygen removal. The effect of γ-alumina on deoxygenation is greater than that of zeolite ZSM-5.

4. Conclusion

In this study, the effects of catalysts (γ-alumina, and zeolite ZSM-5) on the pyrolysis process of castor meal are investigated. The operation conditions are based on the previous study using Taguchi method and the following findings are obtained.

1. Based on the TGA analysis of castor meal, maximum mass loss occurred at 339 °C without a catalyst. Adding zeolite ZSM-5 did not obviously affect the pyrolysis temperature. However, when γ-alumina was added, the major pyrolysis temperature decreased to 284 °C.
2. Catalysts (γ-alumina and zeolite ZSM-5) changed the pyrolysis mode of castor meal. In the early stage of pyrolysis of castor meal, catalysts increased the amounts of H_2O, CH_4, CO_2, CO, and phenol, particularly for γ-alumina. Both catalysts enhanced secondary reactions and volatile substances were decomposed into smaller hydrocarbon molecules, mainly H_2O, CO and CO_2.
3. Based on the TGA burning profiles of pyrolytic products from castor meal, two major peaks represented coal vitrinite combustion and coal inertinite combustion for pyrolytic biochar with 19.55% of the mass left. The combustion of the castor pyrolytic oil inhibited multistage reactions and only 0.049% of the total mass remained as residue.
4. Zeolite ZSM-5 and γ-alumina slightly decreased the pyrolytic oil yield and increased the yield of aqueous substances. Zeolite ZSM-5 increased the yield of castor meal char and γ-alumina increased the yield of pyrolytic gases.
5. Adding catalysts in pyrolysis of castor meal facilitated the decomposition of high-carbon-number pyrolytic oil into low-carbon-number pyrolytic oil. These catalysts also helped remove oxygen, increased the viscosity index, and decreased the viscosity of pyrolytic oil. In addition, for the deoxygenating ability, the effect of γ-alumina was greater than that of zeolite ZSM-5.

Table 4
Elemental analysis and heating values of the pyrolytic oil obtained from castor meal.

	N (%)	C (%)	H (%)	O (%)	Calorific value (MJ/kg)
Catalytic ratio of γ-alumina (wt%)					
0	4.88	52.34	6.24	22.3	22.277
1	5.62	52.84	7.09	23.32	23.106
5	5.42	55.01	8.99	20.43	25.882
10	5.55	54.42	9.45	20.31	26.095
Catalytic ratio of zeolite ZSM-5 (wt%)					
0	4.88	52.34	6.24	22.3	22.277
1	6.21	52.9	8.29	21.69	24.331
5	6.77	53.12	8.33	20.75	24.493
10	6.12	54.02	8.96	21.57	25.362

Acknowledgments

This research was supported by the Ministry of Science and Technology (Republic of China, Taiwan) under Grant numbers MOST 104-ET-E-006-001-ET (G.B. Chen) and MOST 104-2221-E-006 -136 (Y.H. Li).

References

[1] Chen G-B, Li Y-H, Cheng T-S, Chao Y-C. Chemical effect of hydrogen peroxide addition on characteristics of methane–air combustion. Energy 2013;55:564–70.
[2] Starikovskiy A, Aleksandrov N. Plasma-assisted ignition and combustion. Prog Energy Combust Sci 2013;39(1):61–110.
[3] Li Y-H, Hsu H-W, Lien Y-S, Chao Y-C. Design of a novel hydrogen–syngas catalytic mesh combustor. Int J Hydrogen Energy 2009;34(19):8322–8.
[4] Kaminski W, Marszalek J, Ciolkowska A. Renewable energy source—dehydrated ethanol. Chem Eng J 2008;135(1–2):95–102.
[5] Nigam PS, Singh A. Production of liquid biofuels from renewable resources. Prog Energy Combust Sci 2011;37(1):52–68.
[6] Kegl B. NOx and particulate matter (PM) emissions reduction potential by biodiesel usage. Energy & Fuels 2007;21(6):3310–6.
[7] Karagöz S, Bhaskar T, Muto A, Sakata Y, Oshiki T, Kishimoto T. Low-temperature catalytic hydrothermal treatment of wood biomass: analysis of liquid products. Chem Eng J 2005;108(1–2):127–37.
[8] Asadullah M, Rahman MA, Ali MM, Rahman MS, Motin MA, Sultan MB, et al. Production of bio-oil from fixed bed pyrolysis of bagasse. Fuel 2007;86(16):2514–20.
[9] Ferreira LC, Nilsen PJ, Fdz-Polanco F, Pérez-Elvira SI. Biomethane potential of wheat straw: influence of particle size, water impregnation and thermal hydrolysis. Chem Eng J 2014;242:254–9.
[10] Lewandowski I, Clifton-Brown JC, Scurlock JMO, Huisman W. Miscanthus: european experience with a novel energy crop. Biomass Bioenergy 2000;19(4):209–27.
[11] Chen W-H, Lin B-J. Characteristics of products from the pyrolysis of oil palm fiber and its pellets in nitrogen and carbon dioxide atmospheres. Energy 2016;94:569–78.
[12] Nurul Islam M, Nurul Islam M, Rafiqul Alam Beg M, Rofiqul Islam M. Pyrolytic oil from fixed bed pyrolysis of municipal solid waste and its characterization. Renew Energy 2005;30(3):413–20.
[13] Cantrell KB, Ducey T, Ro KS, Hunt PG. Livestock waste-to-bioenergy generation opportunities. Bioresour Technol 2008;99(17):7941–53.
[14] Yang SI, Wu MS, Wu CY. Application of biomass fast pyrolysis part I: pyrolysis characteristics and products. Energy 2014;66:162–71.
[15] Yang SI, Hsu TC, Wu CY, Chen KH, Hsu YL, Li YH. Application of biomass fast pyrolysis part II: the effects that bio-pyrolysis oil has on the performance of

diesel engines. Energy 2014;66:172–80.
[16] Bridgwater AV. Review of fast pyrolysis of biomass and product upgrading. Biomass Bioenergy 2012;38:68–94.
[17] Basu P. Biomass gasification, pyrolysis and torrefaction. Practial Design and Theory Academic press; 2013. Chap. 5.
[18] Figueiredo MKK, Romeiro GA, Damasceno RN. Low temperature conversion (LTC) of castor seeds—a study of the oil fraction (pyrolysis oil). J Anal Appl Pyrolysis 2009;86(1):53–7.
[19] Koufopanos CA, Papayannakos N, Maschio G, Lucchesi A. Modelling of the pyrolysis of biomass particles. Studies on kinetics, thermal and heat transfer effects. Can J Chem Eng 1991;69(4):907–15.
[20] Chen G-L, Chen G-B, Li Y-H, Wu W-T. A study of thermal pyrolysis for castor meal using the Taguchi method. Energy 2014;71:62–70.
[21] Ahmed II , Gupta AK. Pyrolysis and gasification of food waste: syngas characteristics and char gasification kinetics. Appl Energy 2010;87(1):101–8.
[22] Demiral İ, Şensöz S. The effects of different catalysts on the pyrolysis of industrial wastes (olive and hazelnut bagasse). Bioresour Technol 2008;99(17):8002–7.
[23] Pütün E, Uzun BB, Pütün AE. Fixed-bed catalytic pyrolysis of cotton-seed cake: effects of pyrolysis temperature, natural zeolite content and sweeping gas flow rate. Bioresour Technol 2006;97(5):701–10.
[24] Babich IV, van der Hulst M, Lefferts L, Moulijn JA, O'Connor P, Seshan K. Catalytic pyrolysis of microalgae to high-quality liquid bio-fuels. Biomass Bioenergy 2011;35(7):3199–207.
[25] Pütün E. Catalytic pyrolysis of biomass: effects of pyrolysis temperature, sweeping gas flow rate and MgO catalyst. Energy 2010;35(7):2761–6.
[26] Wang P, Zhan S, Yu H, Xue X, Hong N. The effects of temperature and catalysts on the pyrolysis of industrial wastes (herb residue). Bioresour Technol 2010;101(9):3236–41.
[27] Shadangi KP, Mohanty K. Production and characterization of pyrolytic oil by catalytic pyrolysis of Niger seed. Fuel 2014;126:109–15.
[28] Shadangi KP, Mohanty K. Thermal and catalytic pyrolysis of Karanja seed to produce liquid fuel. Fuel 2014;115:434–42.
[29] Koul M, Shadangi KP, Mohanty K. Effect of catalytic vapour cracking on fuel properties and composition of castor seed pyrolytic oil. J Anal Appl Pyrolysis 2016;120:103–9.
[30] Xu G, Zou J, Li G. Ceramsite made with water and wastewater sludge and its characteristics affected by SiO2 and Al2O3. Environ Sci Technol 2008;42(19):7417–23.
[31] Morgan PA, Robertson SD, Unsworth JF. Combustion studies by thermogravimetric analysis. Fuel 1987;66(2):210–5.
[32] Düng NA, Klaewkla R, Wongkasemjit S, Jitkarnka S. Light olefins and light oil production from catalytic pyrolysis of waste tire. J Anal Appl Pyrolysis 2009;86(2):281–6.
[33] Lloyd WG, Davenport DA. Applying thermodynamics to fossil fuels: heats of combustion from elemental compositions. J Chem Educ 1980;57(1):56.